

## Production of pseudoscalar Higgs bosons in $e\gamma$ collisions

Duane A. Dicus

*Center for Particle Physics and Department of Physics, University of Texas, Austin, Texas 78712*

Wayne W. Repko

*Department of Physics and Astronomy, Michigan State University, East Lansing, Michigan 48824*

(Received 6 November 1995)

We investigate the production of a pseudoscalar Higgs boson  $A^0$  using the reaction  $e\gamma \rightarrow eA^0$  at an  $e\bar{e}$  collider with a center-of-mass energy of 500 GeV. Supersymmetric contributions are included which provide a substantial enhancement to the cross section for most values of the symmetry-breaking parameters. We find that, despite the penalty incurred in converting one of the beams into a source of backscattered photons, the  $e\gamma$  process is a promising channel for the detection of the  $A^0$ .

PACS number(s): 14.80.Cp, 12.60.Jv, 13.10.+q

### I. INTRODUCTION

The Higgs sector in supersymmetric extensions of the standard model contains charged Higgs bosons as well as additional neutral Higgs bosons [1]. Among the latter is a pseudoscalar particle usually denoted  $A^0$ . In this paper, we calculate the production cross section for the  $A^0$  in the process  $e\gamma \rightarrow eA^0$ . Contributions to this process arise from triangle and box diagrams. The triangle contributions consist of diagrams in which the  $A^0$  and photon are on-shell external particles and the remaining particle is a virtual photon or  $Z^0$  in the  $t$  channel. Since  $t=0$  is in the physical region, the photon pole contribution dominates the  $Z^0$  pole contribution in this set of diagrams [2]. Moreover, because of the off-diagonal structure of the  $A^0$  couplings to other bosons, the particles in the loop are either quarks, leptons, or charginos. Here, we present the top quark, bottom quark,  $\tau$  lepton and the two chargino contributions to the photon pole amplitude.

The box diagrams have a more complex particle structure, with leptons, charginos, neutralinos, and scalar leptons in the loops. Like the  $Z^0$  pole, these diagrams are nonsingular at  $t=0$ , and should not contribute a sizable correction to the photon pole terms. They are not included in the present calculation.

### II. THE CROSS SECTION FOR $A^0$ PRODUCTION

The amplitude for the production of an  $A^0$  of momentum  $k'$  and an  $e$  of momentum  $p'$  in the collision of an  $e$  of momentum  $p$  and a  $\gamma$  of momentum  $k$  and polarization  $\varepsilon_\lambda(k)$  by the exchange of a  $\gamma$  in the  $t$  channel is

$$\mathcal{M} = \frac{4i\alpha^2}{\sin\theta_W m_W} \bar{u}(p') \gamma_\mu u(p) \frac{\mathcal{A}_\gamma(t)}{t} \varepsilon_{\mu\nu\alpha\beta} \varepsilon_\nu(k) \times (p-p')_\alpha k_\beta, \quad (1)$$

where  $t = -(p-p')^2$ , and

$$\begin{aligned} \mathcal{A}_\gamma(t) = & [-3(\frac{2}{3})^2 m_t^2 \cot\beta C_0(t, m_A^2, m_t^2) \\ & - 3(-\frac{1}{3})^2 m_b^2 \tan\beta C_0(t, m_A^2, m_b^2) \\ & - (-1)^2 m_\tau^2 \tan\beta C_0(t, m_A^2, m_\tau^2) \\ & + 2m_W m_1 g_{11} C_0(t, m_A^2, m_1^2) \\ & + 2m_W m_2 g_{22} C_0(t, m_A^2, m_2^2)]. \quad (2) \end{aligned}$$

Here,  $m_t$  and  $m_b$  are the top and bottom quark masses,  $m_\tau$  is the  $\tau$  lepton mass,  $m_1$  and  $m_2$  are the chargino masses,  $m_W$  is the  $W$  mass, and  $\tan\beta$  is a ratio of vacuum expectation values [1]. The chargino coupling constants  $g_{11}$  and  $g_{22}$  depend on the elements of two  $2 \times 2$  unitary matrices  $U$  and  $V$  which diagonalize the chargino mass matrix  $X$ , where [3]

$$X = \begin{pmatrix} M & \sqrt{2}m_W \sin\beta \\ \sqrt{2}m_W \cos\beta & \mu \end{pmatrix}, \quad (3)$$

and which are chosen to ensure that  $m_1$  and  $m_2$  are positive. For illustrative purposes, we assume that the symmetry-breaking parameters  $M$  and  $\mu$  are real and consider two cases:  $M\mu > m_W^2 \sin 2\beta$  and  $M\mu < m_W^2 \sin 2\beta$ . The couplings in these cases are

$$\begin{aligned} g_{11} &= \frac{m_W}{m_1^2 - m_2^2} (m_2 + m_1 \sin 2\beta), \\ g_{22} &= -\frac{m_W}{m_1^2 - m_2^2} (m_1 + m_2 \sin 2\beta), \quad (4) \end{aligned}$$

for  $M\mu > m_W^2 \sin 2\beta$ , and

$$\begin{aligned} g_{11} &= \frac{m_W}{m_1^2 - m_2^2} (-m_2 + m_1 \sin 2\beta), \\ g_{22} &= -\frac{m_W}{m_1^2 - m_2^2} (-m_1 + m_2 \sin 2\beta), \quad (5) \end{aligned}$$

for  $M\mu < m_W^2 \sin 2\beta$ . Notice that these couplings are symmetric in  $m_1, m_2$  and, unlike the  $A^0$ -top coupling, there is no

enhancement factor of  $m_{1,2}/m_W$  [4]. We take  $m_1 \geq m_2$ . Because of the reality of  $M$  and  $\mu$ ,  $m_1$  and  $m_2$  in Eqs. (4) and (5) are subject to certain constraints discussed below [5]. The scalar function  $C_0(t, m_A^2, m^2)$  is [6]

$$C_0(t, m_A^2, m^2) = \frac{1}{i\pi^2} \int d^4q \frac{1}{(q^2 + m^2)[(q+p-p')^2 + m^2][(q+p-p'+k)^2 + m^2]}. \quad (6)$$

Since one of the external particles is a photon, this function can be expressed in terms of inverse trigonometric or hyperbolic functions [1,7] as

$$C_0(t, m_A^2, m^2) = \frac{1}{(t - m_A^2)} \left[ C\left(\frac{m_A^2}{m^2}\right) - C\left(\frac{t}{m^2}\right) \right], \quad (7)$$

where

$$C(\beta) = \int_0^1 \frac{dx}{x} \ln[1 - \beta x(1-x) - i\varepsilon] \quad (8)$$

$$= \begin{cases} 2 \left[ \operatorname{arcsinh}\left(\sqrt{-\frac{\beta}{4}}\right) \right]^2, & \beta \leq 0, \\ -2 \left[ \operatorname{arcsin}\left(\sqrt{\frac{\beta}{4}}\right) \right]^2, & 0 \leq \beta \leq 4, \\ 2 \left[ \operatorname{arccosh}\left(\sqrt{\frac{\beta}{4}}\right) \right]^2 - \frac{\pi^2}{2} - 2i\pi \operatorname{arccosh}\left(\sqrt{\frac{\beta}{4}}\right), & \beta \geq 4. \end{cases} \quad (9)$$

The cross section is given by

$$\frac{d\sigma(e\gamma \rightarrow eA_0)}{d(-t)} = \frac{1}{64\pi s^2} \sum_{\text{spin}} |\mathcal{M}|^2, \quad (10)$$

and we have

$$\sum_{\text{spin}} |\mathcal{M}|^2 = \frac{\alpha^4}{\sin^2 \theta_W m_W^2} (s^2 + u^2) \frac{|\mathcal{A}_\gamma(t)|^2}{(-t)}, \quad (11)$$

where  $s = -(p+k)^2$  and  $u = -(p'-k)^2$ . The presence of the  $1/t$  in Eq. (11) means it is necessary to introduce a cutoff in the calculation of the total cross section. One approach to obtain a finite cross section is to use the effective photon or Weizsäcker-Williams approximation for the exchanged photon [8]. Here, we integrate the exact amplitude and impose an angular cutoff. The expression for the total cross section is

$$\sigma_{e\gamma \rightarrow eA^0}(s) = \frac{\alpha^4}{64\pi \sin^2 \theta_W m_W^2} \int_{\eta(s-m_A^2)}^{(s-m_A^2)} \frac{dy}{y} \left( 2 - 2 \frac{(m_A^2 + y)}{s} + \frac{(m_A^2 + y)^2}{s^2} \right) |\mathcal{A}_\gamma(-y)|^2, \quad (12)$$

where  $\eta$  is an angular cutoff. We investigated the effect of varying  $\eta = \sin^2(\theta_{\min}/2)$  by comparing the standard model cross section with and without the  $Z^0$  exchange. For  $\theta_{\min}$  as large as  $\pi/6$ , the  $Z^0$  contribution is only 3%–4% of the total. The result scales approximately as the logarithm of  $\eta$ , and we use  $\eta = 10^{-5}$  in the figures.

To complete the calculation of the cross section for the  $e\gamma$  process, it is necessary to fold the cross section, Eq. (12), with the distribution  $F_\gamma(x)$  of backscattered photons having momentum fraction  $x$  [9] to obtain

$$\sigma_T = \frac{1}{s} \int_{m_A^2}^{0.83s} d\hat{s} F_\gamma\left(\frac{\hat{s}}{s}\right) \sigma_{e\gamma \rightarrow eA^0}(\hat{s}), \quad (13)$$

with  $\hat{s} = xs$ . Here, we have taken the usual upper limit on the allowed  $x$  value,  $x = 0.83$ .

This cross section is plotted in Fig. 1 for  $M\mu > m_W^2 \sin 2\beta$  and in Fig. 2 for  $M\mu < m_W^2 \sin 2\beta$ . The dashed line in each panel is the contribution from the top and bottom quarks and the  $\tau$  lepton. For large  $\tan\beta$ , the  $\tau$  contribution is important. This is illustrated in the  $\tan\beta = 20$  panel of Fig. 1, where the dot-dashed line is the contribution from the top and bottom quarks. In Fig. 1, the solid lines are  $m_1 = 250$  GeV and  $m_2$  the largest value consistent with the constraint  $(m_1 - m_2) \geq m_W \sqrt{2(1 + \sin 2\beta)}$ , which is needed to ensure that  $M$  and  $\mu$  are real. Similarly, in Fig. 2, the solid lines correspond to  $m_1 = 250$  GeV and  $m_2$  the largest value consistent with  $(m_1 - m_2) \geq m_W \sqrt{2(1 - \sin 2\beta)}$ . Unlike the  $M\mu > m_W^2 \sin 2\beta$  case, when  $M\mu < m_W^2 \sin 2\beta$ , it is possible for  $m_1$  and  $m_2$  to be equal for  $\tan\beta = 1$  provided the  $m_1, m_2 \geq m_W$ . These values of  $m_1$  and  $m_2$  are within the range of chargino masses found in studies of minimal supersymmetric models [10]. In most cases, the inclusion of the chargino contribution leads to a significant increase in the cross section, especially for the larger values of  $\tan\beta$ .

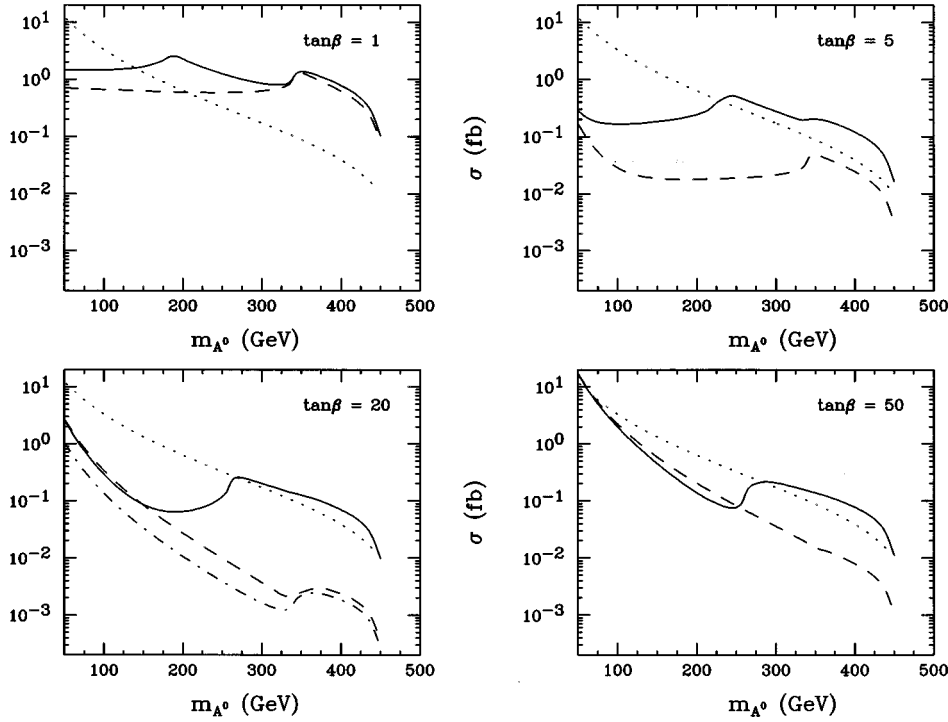


FIG. 1. Cross sections for the production of  $A^0$  are shown for various values of  $\tan\beta$  and an  $e\bar{e}$  center-of-mass energy of 500 GeV when  $M\mu > m_W^2 \sin 2\beta$ . In each case, the solid line corresponds to chargino masses  $m_1 = 250$  GeV and  $m_2$  the largest value consistent with the restriction  $(m_1 - m_2) \geq m_W \sqrt{2(1 + \sin 2\beta)}$ . The dashed line is the standard two Higgs doublet contribution without charginos, and the dot-dashed line in the  $\tan\beta = 20$  panel is the two Higgs doublet result without the  $\tau$  contribution. The dotted lines are the cross sections for the production of a background  $b\bar{b}$  with invariant mass  $m_A$ . In these graphs, the angular cutoff  $\eta$  is taken to be  $10^{-5}$ .

To assess the observability of this process, we assume that the dominant  $A_0$  decay is  $A_0 \rightarrow b\bar{b}$ . For  $m_A < 2m_t$ , this ignores some contribution from chargino pair decay, but this is relatively small since in all but one of the examples we consider, the lowest chargino mass exceeds  $\sim 120$  GeV. Even above the top threshold,  $b\bar{b}$  decay dominates when  $\tan\beta \sim 20$  [11]. The dotted lines in Figs. 1 and 2 are the cross sections for the direct production of a background  $b\bar{b}$  of invariant mass  $m_A$  in  $e\gamma$  collisions subject to an angular cut on the  $b$  and  $\bar{b}$  direction relative to that of the incident pho-

ton in the  $e\gamma$  center of mass. We find that an angular cut of  $|\cos\theta| < 0.98$  on both the  $b$  and the  $\bar{b}$  reduces the background  $b\bar{b}$  cross section by about a factor of 10 while leaving the  $b\bar{b}$  signal from  $A^0$  decay essentially unchanged. More restrictive cuts on the  $b$  and  $\bar{b}$  angles can further suppress the background, but at the expense of a significant decrease in the signal [12]. The cut shown appears to be optimal.

### III. DISCUSSION

We would like to point out that the  $e\gamma$  cross sections calculated here are very likely to be much larger than those

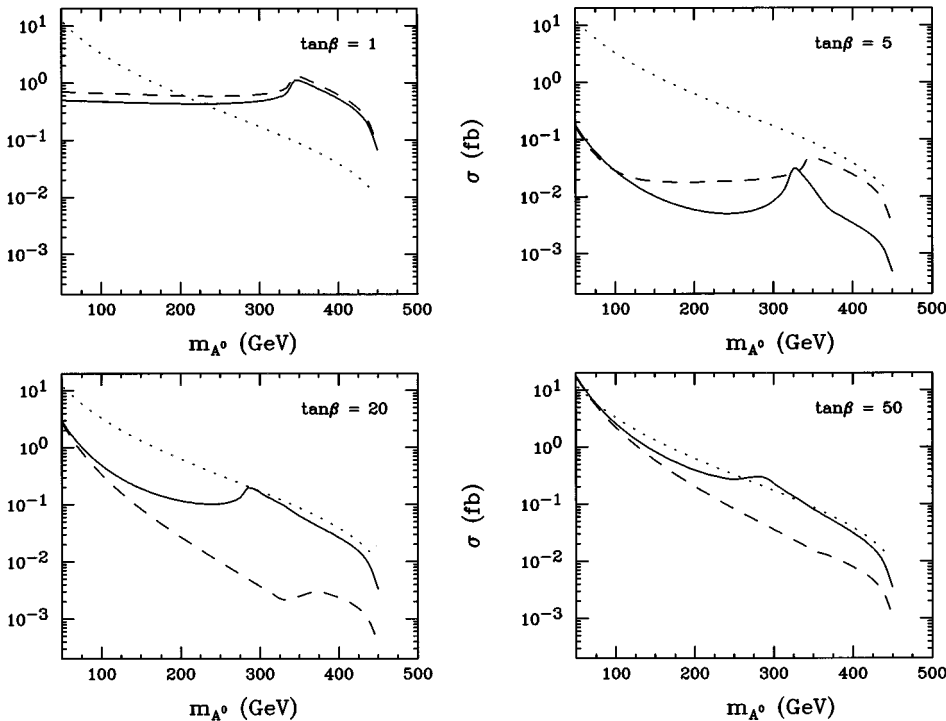


FIG. 2. Same as Fig. 1 for  $M\mu < m_W^2 \sin 2\beta$ . In this case,  $m_1$  and  $m_2$  satisfy the condition  $(m_1 - m_2) \geq m_W \sqrt{2(1 - \sin 2\beta)}$ .

of the related process  $e\bar{e} \rightarrow \gamma A^0$  at 500 GeV. We have checked this for the production of the standard model Higgs boson using the complete (standard model) calculation of  $e\bar{e} \rightarrow \gamma H^0$  [7] and the photon pole contribution to  $e\gamma \rightarrow eH^0$ . At an  $e\bar{e}$  center-of-mass energy of 500 GeV, we find the cross section  $\sigma(e\bar{e} \rightarrow \gamma H^0)$  for the production of a 200 GeV  $H^0$  is 0.08 fb, whereas  $\sigma(e\gamma \rightarrow eH^0) = 5.9$  fb for the same Higgs-boson mass.

This enhancement is implicit in a previous calculation of scalar Higgs-boson production [8] where the Weizsäcker-Williams approximation is used for the  $t$ -channel photon together with the on-shell  $H \rightarrow \gamma\gamma$  amplitude. This is essentially equivalent to setting  $y=0$  in the parentheses of Eq. (12) and using  $m_e^2$  as the cutoff in the remaining integral [13]. Our comparison of the approximate results of Ref. [8] with an exact calculation suggests that the Weizsäcker-Williams approach tends to overestimate the cross section. Apart from minor variations depending on how the calculation is performed, it is nevertheless true that the  $t$ -channel cross section is substantially larger than its  $s$ -channel counterpart.

The production of  $A^0$  has also been investigated in  $\gamma\gamma$

collisions [14]. In that case, the background arises from the process  $\gamma\gamma \rightarrow b\bar{b}$  and it is effectively suppressed by imposing an angular cut. With our choice of chargino masses, a comparison of the  $\tan\beta=20$  cross sections in  $e\gamma$  production and  $\gamma\gamma$  production [14] reveals a larger signal in the  $e\gamma$  mode. Both channels are likely to be important in searches for the  $A^0$ .

To the extent that the photon pole contribution can be isolated, this method of searching for the  $A^0$  has the advantage that the contributions from supersymmetry are significant and limited to one type of supersymmetric particle. Should one observe a cross section larger than any standard model prediction, the case for the presence of chargino contributions is rather strong.

#### ACKNOWLEDGMENTS

We would like to thank C.-P. Yuan and X. Tata for conversations. This research was supported in part by the National Science Foundation under Grant No. PHY-93-07980 and by the United States Department of Energy under Contract No. DE-FG013-93ER40757.

- 
- [1] J. F. Gunion, H. E. Haber, G. Kane, and S. Dawson, *The Higgs Hunter's Guide* (Addison-Wesley, Menlo Park, CA, 1990).
  - [2] The same thing can be said about the production of scalar Higgs bosons in the reaction  $e\gamma \rightarrow eH^0$ .
  - [3] J. F. Gunion and H. E. Haber, Nucl. Phys. **B272**, 1 (1986).
  - [4] H. Baer, A. Bartl, D. Karatas, W. Majerotto, and X. Tata, Int. J. Mod. Phys. A **4**, 4111 (1989), Appendix B.
  - [5] X. Tata and D. A. Dicus, Phys. Rev. D **35**, 2110 (1987).
  - [6] G. 't Hooft and M. Veltman, Nucl. Phys. **B153**, 365 (1979).
  - [7] A. Abbasabadi, D. Bowser-Chao, D. A. Dicus, and W. W. Repko, Phys. Rev D **52**, 3919 (1995).
  - [8] O. J. P. Éboli, M. C. Gonzalez-Garcia, and S. F. Novaes, Phys. Rev. D **49**, 91 (1994).
  - [9] I. F. Ginzburg, G. L. Kotkin, S. L. Panfil, V. G. Serbo, and V. I. Telnov, Nucl. Instrum. Methods Phys. Res. Sect. A **219**, 5 (1984).
  - [10] G. L. Kane, C. Kolda, L. Roszkowski, and J. D. Wells, Phys. Rev. D **49**, 6173 (1994).
  - [11] V. Barger, K. Cheung, R. J. N. Phillips, and A. L. Stange, Phys. Rev. D **46**, 4914 (1992).
  - [12] If the  $A^0$  mass should turn out to be very close to the  $Z$  mass, there could be a substantial background from  $\gamma e \rightarrow Ze \rightarrow b\bar{b}e$ . We have not included this in our background calculation.
  - [13] To see this in detail, compare the simplified Eq. (12) with Eq. (4) of Ref. [8].
  - [14] J. F. Gunion and H. E. Haber, Phys. Rev. D **48**, 5109 (1993).